Determination of Polymer Effective Charge by Indirect UV Detection in Capillary Electrophoresis: Toward the Characterization of Macromolecular Architectures

Nadia Anik,[†] Marc Airiau,[‡] Marie-Pierre Labeau,[§] Chi-Thanh Vuong,[‡] Julien Reboul,[||] Patrick Lacroix-Desmazes,[||] Corine Gérardin,[||] and Hervé Cottet*,[†]

Institut des Biomolécules Max Mousseron (IBMM, UMR 5247 CNRS−Université de Montpellier 1−Université de Montpellier 2), place Eugène Bataillon, case courrier 1706, 34095 Montpellier Cedex 5, France; Rhodia Opérations, 52 rue de la haie Coq, 93308 Aubervilliers, France; Rhodia Inc., 350 G. Patterson Bvd, Bristol, Pennsylvania 19007; and Institut Charles Gerhardt (UMR 5253 CNRS−ENSCM−Université de Montpellier 1−Université de Montpellier 2) 8, rue de l'Ecole Normale, 34296 Montpellier Cedex 5, France

Received November 8, 2008; Revised Manuscript Received January 20, 2009

ABSTRACT: This work deals with the determination of polymer effective charge based on the sensitivity of detection in capillary electrophoresis using indirect UV detection. In this detection mode, the polyelectrolyte (solute) displaces a certain quantity of probe contained in the background electrolyte and having the same charge as the solute. This quantity of displaced probe is directly correlated to the effective charge of the solute. Contrary to other electrophoretic methods generally used for monitoring changes in effective charge, this methodology is not based on the effective mobility of the polyelectrolyte (i.e., migration times) but on the sensitivity of detection (i.e., peak areas). Experimental values of effective charge obtained for statistical copolymers of poly(acrylamide-*co*-sodium 2-acrylamido-2-methylpropanesulfonate), for homopolymers of poly(diallyldimethylammonium chloride), poly(acrylic acid), and poly(metacrylic acid), are compared to the Manning theory of charge condensation. Interestingly, this methodology can be used for the characterization of macromolecular architecture since the effective charge of copolymers highly depends on the repartition of the charged monomers along the polymer chain. As an example, this methodology can easily distinguish statistical copolymers from diblock copolymers of similar chemical charge densities. Experiments were carried out on diblock copolymers of poly(acrylic acid)-*b*-poly(ethylene oxide) (PAA-*b*-PEO) and poly(methacrylic acid)-*b*-poly(ethylene oxide) (PMAA-*b*-PEO). The variation of the sensitivity of detection of statistically charged copolymers in the indirect UV mode with the chemical charge density is also discussed in detail.

1. Introduction

Polyelectrolytes are widely used for industrial applications, ranging from stabilization or flocculation of suspensions to tailoring charge and hydrophobicity of solid surfaces. These widespread applications are based on the ability of polyelectrolytes to interact with surfaces or (macro)molecules. The binding of polyelectrolytes to oppositely charged proteins,[1,2] dendrimers,[3] or polymers[4] has attracted extensive investigations because of its importance in industrial processes and biological systems. For example, numerous studies on complex formation between two polyelectrolytes of opposite charges have been motivated by interest in various applications such as microencapsulation,[5] membranes with special separation properties,[6] flocculants for colloidal dispersions,[7] surface modification of silicate powder,[8] templating of mesostructured inorganic materials,[9] or sorption of organic molecules in wastewater cleaning.[10] Since the charges of polyelectrolytes are one of the driving forces for adsorption and binding, knowledge of the effective charge of polyelectrolytes in solution is an important issue.[11]

Capillary electrophoresis (CE) is a powerful tool for separating and characterizing charged polymers,[12,13] including two-dimensional approaches.[14,15] It is now well-known that free-solution capillary electrophoresis (FSCE) has the potential to separate polyelectrolytes according to their charge density, as far as this charge density is lower than the threshold value above which counterion condensation occurs. The term "free solution" means that the separation is performed in the absence of sieving matrix (gel or entangled polymer solution). The variation of free solution electrophoretic mobility with chemical charge density was first examined by Hoagland et al.[16] on copolymers of acrylic acid (AA) and acrylamide (AM). They found that the electrophoretic mobility tends to level off above the critical charge density predicted by Manning.[17] For a vinyl polyelectrolyte, this critical charge density corresponds to a chemical composition of 36 mol % of charged monomers. Other papers on the same topic but on different copolymers confirmed these findings. Gao et al.[18] studied statistical copolymers of 2-acrylamido-2-methylpropanesulfonate (AMPS) and acrylamide (AM). They confirmed the presence of a threshold in mobility above 36% charge density. However, they reported a slight increase of the mobility above this critical value. Staggemeier et al.[19] confirmed by frontal analysis continuous capillary electrophoresis (FACCE) the counterion condensation on statistical copolymers of PAMAMPS and indicated that the electrophoretic mobility distribution could be related to the distribution in chemical composition. For that, they demonstrated that the electrophoretic mobility distribution of hyaluronic acid (HA), which is a homogeneous copolymer in terms of chemical composition, was much less disperse than for statistical PAM-AMPS. Zhang et al.[20] used the same approach to observe the compositional heterogeneity of commercial samples of poly(styrenesulfonate) (PSS) and demonstrated that samples synthesized by sulfonation of polystyrene were much more heterogeneous in chemical composition than those prepared by

* Corresponding author: Tel +33 4 6714 3427; Fax +33 4 6763 1046; e-mail hcottet@univ-montp2.fr.
[†] Institut des Biomolécules Max Mousseron.
[‡] Rhodia Opérations.
[§] Rhodia Inc.
[||] Institut Charles Gerhardt.

10.1021/ma8025095 CCC: $40.75
Published on Web 03/23/2009

polymerization of styrenesulfonate. Other examples of CE applications to polyelectrolyte characterization are given by Oudhoff et al.,[21] who used electrophoretic mobility distributions for the determination of the degree of substitution of carboxymethylcellulose. Pieric et al.[22] also suggested that the electropherogram peak width indicated polydispersity in composition for AA/AM copolymers. Popov et al.[23] used CE to describe the counterion condensation mechanism from electrophoretic mobility measurements. They carried out a systematic CE study in order to understand the variation of the polyelectrolyte effective charge density ξ_{eff} as a function of the distance between the charge along the chain, b, and the solvent dielectric constant, ε_r.

Other experimental techniques were used for investigating Manning condensation. Essafi et al.[24] demonstrated by SAXS and SANS that Manning counterion condensation leads to a renormalization of the charge density. The scattering function is invariant with the chemical charge density (f) above the value of $f = 0.4$. SANS measurements were also carried out by Von Klitzing et al.[25] for statistical copolymers of diallyldimethylammonium chloride (DADMAC) and *N*-methyl-*N*-vinylacetamide (NMVA) of different charge densities. The position of the scattering function was affected by the charge density up to a threshold value of $f = 0.5$. However, there was no value between $f = 0.5$ and 1 to accurately determine the counterion condensation threshold. Pochard et al.[26] gave evidence of Manning condensation by conductometric measurements on poly(acrylic acid) (PAA).

The direct determination of the effective charge density (f_{eff}) of polyelectrolytes remains a challenging issue. f_{eff} depends on the chemical charge density (f), the degree of dissociation, and the degree of counterion condensation.[27] Direct potentiometry using ion selective electrodes can be used to determine the effective charge density of polyelectrolytes.[28−33] The limitation of this method is the availability and selectivity of the appropriate ion selective electrodes. Other existing methods are generally not straightforward. They are based on the determination of related parameters such as the electrophoretic mobility, the conductivity, or the osmotic pressure[34] but not on the direct determination of the effective charge. Many of these indirect procedures are based on the difference of the mobility between free and condensed counterions.[35−37] Recently, Bôhme et al.[38−40] determined effective charge by dynamic NMR. However, this procedure is based on the assumption that the hydrodynamic friction coefficient (determined from the diffusion coefficient measured by pulsed-field gradient NMR) is equal to the electrophoretic friction coefficient (which is related to the electrophoretic mobility determined by electrophoresis NMR). This holds true only for small charged molecules or oligomers having typical dimensions smaller than the Debye length.[41]

Another challenging issue in the characterization of charged copolymers is the knowledge of the distribution in monomers along the polyelectrolyte chain, which primarily results from the kinetics of reaction. The traditional procedure to get the instantaneous and average copolymer composition during a polymerization process is based on the knowledge of the monomer reactivity ratios.[42] Even if macromolecular microstructure/sequence distribution can be calculated from the reactivity ratios,[43−45] the measurement of the effective charge brings direct information on the distribution of the monomers along the chain. The first objective of the present work is to propose a new methodology for the determination of the polymer effective charge based on the measurement of the sensitivity of detection in indirect UV detection CE. Applying this approach to a series of polyelectrolytes differing in charge densities and/or monomer distributions (statistical versus block copolymers), a second objective of this work is to demonstrate the possibility to get information on the monomer distribution by comparing the experimental polymer effective charge to the theoretical value predicted by Manning theory. Finally, the sensitivity of detection of statistical copolymers in the indirect UV detection mode as a function of the chemical charge density is also discussed in detail.

2. Theoretical Background

2.1. Indirect UV Detection Mode and Transfer Ratio. Indirect UV detection was first introduced in CE by Hjerten et al. in 1987.[46] In this detection mode, an absorbing co-ion (an ion with the same charge as the solute), called the probe, is added to the background electrolyte (BGE). The indirect detection is due to the displacement of the probe by the solute leading to a decrease in the background absorbance. Therefore, a negative signal is recorded when the sample zone passes in front of the detector. The ability of the solute to displace the probe is directly related to the transfer ratio (TR), also called the displacement ratio or response factor, which is defined as the number of moles of the probe displaced by mole of solutes. The signal response Abs in the sample zone is given by

$$\mathrm{Abs} = \varepsilon l \mathrm{TR} C_S \tag{1}$$

where ε is the molar extinction coefficient of the probe at the detection wavelength, l is the optical path length, and C_S is the molar concentration of the sample.

The Kohlraush regulating function (KRF) as derived by Kohlraush[47] is a conservation law. KRF is based on a balance of ion fluxes at the moving sample boundaries and on the principle of electroneutrality, in the absence of molecular diffusion. KRF is constant throughout the electrophoretic run at a given axial coordinate x along the capillary. In an electric field, the migration of charge species from separate moving zones are governed by the KRF:

$$\sum \frac{z_i C_i}{\mu_i} = w(x) \tag{2}$$

where C_i, z_i, and μ_i represent ionic concentrations, absolute value of the charge and effective mobilities of all ionic constituents, respectively. From KRF, it can be shown[48] that the change in concentration (ΔC_A) in probe ion (A) caused by the solute (S) at concentration C_S is given by the transfer ratio (TR):

$$\mathrm{TR} = \frac{|\Delta C_A|}{C_S^S} = \frac{z_S}{z_A} \frac{\mu_A(\mu_S + \mu_C)}{\mu_S(\mu_A + \mu_C)} \tag{3}$$

where z_A and z_S are respectively the effective charges of the probe and solute, and μ_A, μ_S, and μ_C are respectively the absolute values of effective mobilities of the probe, the solute, and the counterion. In the case of a polyelectrolyte chain, the effective charge density z_S corresponds to the charge of the polyelectrolyte chains with its condensed counterions, constituting a single well-defined molecular species. Experimentally, TR values can be calculated according to Doble et al.[49] by determining the following ratio:

$$\mathrm{TR} = \frac{\alpha_S}{\alpha_A} \tag{4}$$

where α_S is the slope of the calibration plot of the solute in indirect UV detection mode and α_A is the slope of the calibration plot of the probe determined by direct UV detection at the same detection wavelength than that used for the solute calibration. Combining eqs 3 and 4, the ratio of charges between the solute and the probe is given by

$$\frac{z_S}{z_A} = \frac{\mu_S[\mu_A + \mu_C]}{\mu_A[\mu_S + \mu_C]} \frac{\alpha_S}{\alpha_A} \quad (5)$$

When the probe is a fully and singly charged small molecule ($z_A = 1$), the effective charge of the solute is directly obtained by

$$z_S = \frac{1}{k_A} \frac{\alpha_S}{\alpha_A} \quad (6)$$

with

$$k_A = \frac{\mu_A[\mu_S + \mu_C]}{\mu_S[\mu_A + \mu_C]} \quad (7)$$

k_A is the mobility ratio that can be easily determined from experimental effective mobilities and/or by correcting limiting mobility values from the effect of ionic strength.

2.2. Indirect UV Detection of Polyelectrolytes. The effective mobility of the species x is determined from the apparent mobility by subtracting the electroosmotic contribution. α_S is the slope of the calibration plot obtained by plotting the time-corrected peak area of the solute versus its molar concentration. When the solute is a polyelectrolyte with possibly different kinds of monomers (charged or uncharged), one has to clearly define what is the molar concentration of the solute. In this work, we found more convenient to consider the molar concentration in charged monomers instead of considering the molar concentration in polyelectrolyte chain.

2.2.1. Charged Copolymers. Let us consider a copolymer that is composed of two different monomers: a charged monomer, noted monomer 1, and an uncharged monomer, noted monomer 2. In that case, the molar concentration in charged monomers $C_{M,1}$ is given by the equation

$$C_{M,1} = \frac{C_{m,polymer} F_1}{M_1} \quad (8)$$

where $C_{m,polymer}$ is the mass concentration in copolymer, F_1 is the mass fraction of charged monomers in the copolymer, and M_1 is the molar mass of a charged monomer. F_1 is related to the molar fraction f of charged monomer in the copolymer by

$$F_1 = \frac{fM_1}{fM_1 + (1-f)M_2} \quad (9)$$

where M_2 is the molar mass of the uncharged monomer. Replacing the expression of F_1 in eq 8 leads to

$$C_{M,1} = \frac{C_{m,polymer} f}{fM_1 + (1-f)M_2} \quad (10)$$

By definition, the molar fraction of charged monomers f, also called the chemical charge density, is expressed as

$$f = \frac{N_1}{N_1 + N_2} \quad (11)$$

where N_1 is the number of moles of charged monomers and N_2 is the number of moles of uncharged monomers in the copolymer sample. Applying eq 6 to the copolymer sample, one can determine the effective charge per charged monomer z_1 as

$$z_1 = \frac{1}{k_A} TR = \frac{1}{k_A} \frac{\alpha_S}{\alpha_A} \quad (12)$$

where α_S is the slope of the calibration plot obtained by plotting the time-corrected peak area of the copolymer versus the molar concentration in charged monomers $C_{M,1}$.

2.2.2. Charged Homopolymers. For homopolyelectrolytes, all the monomers (noted monomers 1) are identical and charged. As in the case of copolymers, the experimental effective charge per monomer z_1 is determined by eq 12. The calibration slope is obtained using the molar concentration in monomer given by

$$C_{M,1} = \frac{C_{m,polymer}}{M_1} \quad (13)$$

2.2.3. Determination of the Effective Charge Density. The average effective charge density f_{eff} of the polyelectrolyte can be determined experimentally from the effective charge per charged monomer z_1 according to

$$f_{eff} = fz_1 \quad (14)$$

This experimental value can be compared to the theoretical one predicted by Manning theory (see next section).

2.3. Counterion Condensation: Manning Theory. Interactions between polyions and small ions in solution are generally described by the Manning limiting laws of counterion condensation.[17] Within this model, the polyion is always assumed to be an infinitely long rigid rod with equally spaced charged (spacing, b), and a fraction of counterions is electrostatically bound or condensed to the polyion, reducing the chemical charge density (f) into an effective charge density (f_{eff}) in solution. This condensation effect is controlled by the interplay of electrostatic and entropic forces. The minimal distance between two unscreened (or uncondensed) charges for which the electrostatic interaction equals the thermal energy kT is called the Bjerrum length l_b and is given by

$$l_b = \frac{e^2}{4\pi\varepsilon_0\varepsilon_r kT} \quad (15)$$

where e is the elementary charge, ε_r is the relative dielectric constant of the solvent, ε_0 is the permittivity of the vacuum, k is the Boltzmann constant, and T is the absolute temperature. In water, at 298 K, l_b is 0.713 nm. The crucial parameter for counterion condensation is the ratio of the Bjerrum length to the charge spacing b, called the Manning parameter or the linear charge density parameter:

$$\xi = \frac{l_b}{b} \quad (16)$$

The linear charge density parameter of a vinyl polymer with a charge spacing of 2.55 Å is $\xi = 2.8$. Values of ξ for statistical vinyl copolymers with different chemical charge densities f (i.e., with an average charge spacing of b/f) can be obtained by multiplying 2.8 by the chemical charge density f. The Manning theory predicts that there is a critical value $\xi_{crit} = 1$, above which counterion condensation occurs. For $\xi < \xi_{crit}$, no condensation takes place, and the effective charge density f_{eff} equals the chemical charge density f. In that case, the effective charge density and the electrophoretic mobility increase linearly with f. For $\xi > \xi_{crit}$, counterion condensation occurs on the polyion surface so that the effective charge density f_{eff} remains equal to the critical value f_{crit} for which $\xi = 1$. For vinyl polymers, f_{crit} equals 0.36. Polyelectrolytes with $f > f_{crit}$ are expected to have an effective charge density and an electrophoretic mobility independent of the chemical charge density f.

3. Experimental Part

3.1. Chemicals. Creatinine and didodecyldimethylammonium bromide (DDAB) were purchased from Aldrich (Milwaukee, WI). Orthophosphoric acid (85%) was from Prolabo (Paris, France). Ammediol was from Avocado (Heysham, England). *p*-Anisic acid was from Aldrich (Steinheim, Germany). Acetic acid was from

Fluka (Seelze, Germany). Deionized water was further purified with a Milli-Q system from Millipore (Molsheim, France).

3.2. Polymers. Statistical copolymers (PAMAMPS) with AMPS molar fraction (or chemical charge density *f*) of 3, 10, 20, 55, 85, and 100% were synthesized to high conversion, at room temperature, by radical polymerization initiated by potassium persulfate and *N,N,N′,N′*-tetramethylethylenediamine (TMEDA) according to the procedure described by McCormick.[14,34] The mean composition of the copolymer measured by proton NMR (3.75 g/L copolymer solution in D_2O) was close to the monomer feed compositions, indicating high conversion. The average molar masses of the PAMAMPS ($M_w \sim 2.5 \times 10^5$ g /mol) were evaluated by aqueous SEC using poly(ethylene oxide) standards for the calibration. Statistical PAMAMPS copolymers with AMPS molar fraction of 30% was from Rhodia (Aubervilliers, France). The polymer was obtained by controlled free-radical polymerization via MADIX.[50,51] The process used was a batch process in ethanol/water mixture (5/95 v/v) with all the monomers and MADIX's transfer agent (xanthate) put in the reactor at the beginning at room temperature. The reaction was performed at 75 °C with several additions of initiator over 5 h. Once the polymerization finalized, ethanol was removed from the mixture under vacuum. The average molar mass of the 30% PAMAMPS ($M_w \sim 6 \times 10^4$ g /mol) was evaluated by aqueous SEC. Diblock copolymers of poly(acrylic acid)-*b*-poly(ethylene oxide) (PAA-*b*-PEO) ($M_{wPAA} \sim$ 4600 g/mol; $M_{wPEO} \sim$ 2000 g/mol) were synthesized by ATRP polymerization according to the procedure described in a previous paper.[52] Poly(methacrylic acid)-*b*-poly(ethylene oxide) (PMAA-*b*-PEO) ($M_{wPMAA} \sim$ 3000 g/mol; $M_{wPEO} \sim$ 8000 g/mol) was purchased from Polymer Source. Poly(methacrylic acid) homopolymers (PMAA) ($M_w \sim$ 75 000 g/mol) was purchased from Fluka (Steinheim, Germany). Poly(acrylic acid) homopolymers (PAA) ($M_w \sim$ 15 000 g/mol) were from Aldrich (Steinheim, Germany). Poly(diallyldimethylammonium chloride) homopolymers (PDADMAC) ($M_w \sim 3.3 \times 10^5$ g/mol) was from Aldrich (Steinheim, Germany).

3.3. Capillary Electrophoresis. CE was carried out with an Agilent Technologies system (Waldbronn, Germany) equipped with a diode array detector. Separation capillaries prepared from bare silica tubing were purchased from Composite Metal Services (Worcester, UK). Capillary dimensions were 33.5 cm (25 cm to the detector) × 50 μm for all analysis unless otherwise specified. New capillaries were conditioned by performing the following washes: 1 M NaOH for 20 min, 0.1 M NaOH for 15 min, and water for 10 min. Between two runs, the capillary was washed 5 min by the electrolyte (1 bar). For the characterization of PDADMAC, DDAB-coated capillary was used. The capillary was flushed between two runs with 0.25 mM DDAB solution (3 min, 1 bar) and electrolyte (2 min, 1 bar). The temperature of the capillary cassette was maintained constant at 25 °C. Polymer samples were prepared in deionized water. Sample volumes of ~4 nL were injected hydrodynamically (17 mbar, 5 s), and a plug of electrolyte was added (10 mbar, 3 s) after the sample zone to improve the repetability. The prepunchers and electrodes were cleaned each 2 days to remove solid deposits. Data were collected at 191, 248, or 254 nm depending on the electrolyte (see caption of the figures).

Electroosmotic mobility was calculated from the migration time of mesityl oxide (neutral marker). Electropherograms were plotted in effective mobility scale (μ_{ep}) using the following equation:

$$\mu_{ep} = \mu_{app} - \mu_{eo} = \frac{lL}{Vt_{app}} - \frac{lL}{Vt_{eo}} \quad (17)$$

where l is the effective length up to the detection point, L the total length of the capillary, V the applied voltage, t_{app} the apparent detection time, and t_{eo} the detection time of the neutral marker.

Curve fittings for the determination of the sensitivity of detection in indirect UV detection mode were performed using the Origin scientific graphing and analysis software (OriginLab, Northampton, MA).

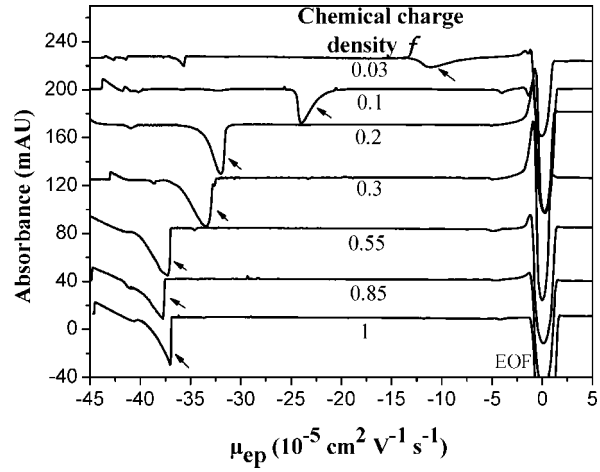

Figure 1. Effective mobility-scale electropherograms obtained for PAMAMPS copolymers of different chemical charge densities *f* using indirect UV detection mode. Electrophoretic conditions: fused-silica capillary, 50 μm i.d. × 33.5 cm (effective length, 25 cm). Electrolyte: 12 mM ammediol, 6 mM *p*-anisic acid, pH 8.8. Applied voltage: +10 kV. Hydrodynamic injection: 17 mbar, 5 s (sample) + 10 mbar, 3 s (electrolyte). Temperature: 25 °C. Samples: PAMAMPS copolymer at 2 g/L in water. The chemical charge density *f* is indicated in the figure. Indirect UV detection at 254 nm. Polymer signal is indicated with an arrow.

4. Results and Discussion

4.1. Indirect UV Detection of PAMAMPS Copolymers in CE. The superposition of the effective mobility-scale electropherograms obtained by indirect UV detection for seven statistical PAMAMPS copolymers of different chemical charge densities *f* varying from 3% to 100% is displayed in Figure 1. Negative peaks indicated with arrows are detected in this background electrolyte containing anisate chromophore and ammediol counterion for indirect UV detection at 254 nm. At this wavelength, PAMAMPS copolymers do not absorb. Since all the PAMAMPS copolymers have relatively high molar masses, the electrophoretic mobility in free solution is independent of the molar mass. Therefore, differences in effective mobility observed between copolymers are directly correlated to the change in effective charge density. As predicted by the Manning theory, and as previously observed,[14,16,18] the effective mobility increases with the chemical charge density up to a critical value of $0.3 < f \leq 0.55$. This observation is in good agreement with the theoretical critical value of $f_{crit} = 0.36$. Above f_{crit}, the mobility becomes almost independent of *f*. It is worth noting that the shape of the polyelectrolyte peaks should be directly correlated to the charge density distribution of the copolymers. However, the electromigration dispersion (EMD), sometimes called overloading effect, can also contribute to the peak asymmetry. In the case of $f = 1$ homopolymer, the asymmetry of the peak is only due to EMD since there is no charge density distribution. The effect of EMD increases with the difference between the mobility of the co-ion and the solute. It also increases with the injected solute concentration. In the present work, the peak shape is not an issue since all measurements are based on the peak area (whatever the shape).

4.2. Determination of the Effective Charge per AMPS Monomer (z_1). To determine the effective charge per AMPS monomer (z_1) in each PAMAMPS copolymer according to eq 12, the sensitivity of detection (α_S) in indirect UV mode has been calculated at 254 nm by plotting the time-corrected area of the copolymer peak as a function of the molar concentration in AMPS monomer $C_{M,1}$ (see Figure 2). It is clearly observed that for $C_{M,1}$ between 1 and 10 mM the time-corrected area varies linearly with $C_{M,1}$. These calibration curves should hit

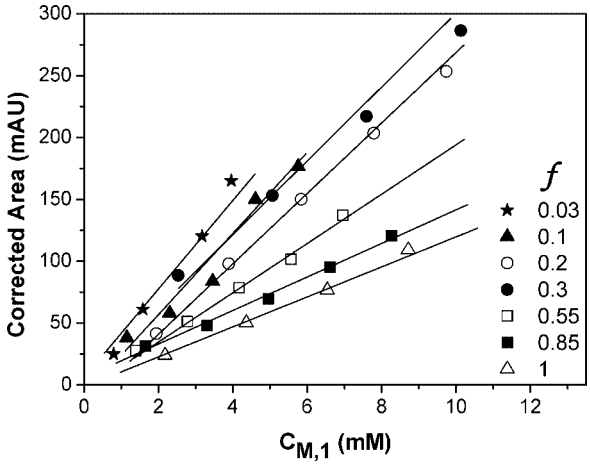

Figure 2. Calibration curves obtained by indirect UV detection CE for PAMAMPS copolymers of different chemical charge densities. Electrophoretic conditions as in Figure 1. $C_{M,1}$ is the molar concentration in charged monomers (AMPS) in the copolymer sample. Each data point is the average of nine measurements. Least squares regression equations: $y = 42.83x - 12.24$ ($r^2 = 0.975$) for $f = 0.03$; $y = 32.03x - 9.42$ ($r^2 = 0.957$) for $f = 0.1$; $y = 27.19x - 9.68$ ($r^2 = 0.999$) for $f = 0.2$; $y = 27.12x + 15.92$ ($r^2 = 0.998$) for $f = 0.3$; $y = 19.31x - 1.37$ ($r^2 = 0.994$) for $f = 0.55$; $y = 13.62x + 5.22$ ($r^2 = 0.992$) for $f = 0.85$; $y = 11.42x + 3.19$ ($r^2 = 0.999$) for $f = 1$.

the origin. This is not strictly the case experimentally, likely due to the lack of precision relative to the drawing of the baseline. Figure 2 also demonstrates that α_S (slope of the lines in Figure 2) depends on the chemical charge density f, as it is discussed in the next section. To get z_1 values using eq 12, the slope (α_A) of the calibration curve of the probe (anisate) was determined at 254 nm using a suitable UV-transparent electrolyte (12 mM ammediol and 6 mM acetic acid, pH 8.8) having the same ionic strength as the background electrolyte used for the indirect UV detection. Transfer ratios TR, which correspond to the number of moles of chromophore displaced by mole of AMPS monomer, were calculated according to eq 4 and are reported in Table 1 with the mobility ratio k_A and the effective charge per AMPS monomer z_1. Mobility ratios k_A were calculated according to eq 7, taking the average effective mobilities calculated by integration of each PAMAMPS peak for μ_S (see Table 1), -28.86×10^{-5} cm^2 V^{-1} s^{-1} for μ_A (determined experimentally in the previously mentioned ammediol/acetic acid buffer) and 28.37×10^{-5} cm^2 V^{-1} s^{-1} for μ_C (calculated from the limiting mobility of ammediol after correction of the ionic strength effect). Finally, z_1 values are plotted in Figure 3 as a function of f (triangles) and were compared to the theoretical values (solid line) from Manning theory. For $f < f_{crit}$, no condensation should occur and z_1 should be constant and equal to 1. For $f > f_{crit}$, condensation should appear, and z_1 should decrease with f ($z_1 = f_{crit}/f$). Experimentally, the decrease of z_1 for $f > 0.36$ is clearly observed, and the three experimental data points are in very good agreement with the theory. For $f < f_{crit}$, experimental z_1 values are constant but lower ($z_1 \sim 0.78$) than the theoretical value ($z_1 = 1$). This discrepancy can be explained by the existence of AMPS sequences in the PAMAMPS chains which are condensed and which decrease the effective charge density.[53] Indeed, the composition drift in copolymerization of AM and AMPS, due to $r_{AM} = 1.0$ and $r_{AMPS} = 0.4$,[54,55] favors the formation of AMPS-rich copolymer chains with AMPS sequences at high conversion. The presence of these sequences could also explain the gradual increase of effective mobility with f as compared to the abrupt increase predicted by the Manning theory. It shows the limitations of these PAMAMPS copolymers to verify the theory. Copolymers with reactivity ratios r (charged monomer) < 1 (to limit sequences of charged monomers) as in the present case but additionally with $r_1 \cong r_2$ (to limit composition drift) would probably better match the theoretical values. It is worth noting that this methodology allowing the direct determination of the polymer effective charge is based on the sensitivity of detection (i.e., peak areas) and not on the effective mobility of the polyelectrolyte (i.e., migration times).

4.3. Variation of the Sensitivity of Detection (α_S) and the Time-Corrected Peak Area (CA) with the Chemical Charge Density *f*. Figure 3 displays the variation of the detection sensitivity α_S (dashed line) as a function of the chemical charge density f. As seen in Figure 2, the sensitivity of detection decreases with f. Theoretically, from eq 12, α_S can be expressed as

$$\alpha_S = z_1 k_A \alpha_A \tag{18}$$

α_A is a constant that does not depend on f. For $f < f_{crit}$, $z_1 = 1$ and therefore α_S scales as k_A, which is a decreasing function of f. For $f > f_{crit}$, k_A becomes independent of f (since μ_S was found to be almost constant) and $z_1 = f_{crit}/f$. Consequently, for $f > f_{crit}$, α_S scales as $1/f$. To sum up, the sensitivity of detection α_S drops with f below f_{crit} because of the decreasing of the mobility ratio k_A, while it decreases above f_{crit} because of the counterion condensation. Experimentally, the three data points above f_{crit} are in very good agreement with the theory while some discrepancies are found below f_{crit} for the same reason as that discussed for the z_1 values.

Experimentally, solutions of polymer samples are often prepared at constant mass concentration $C_{m,polymer}$, as for the experimental conditions of Figure 1 where $C_{m,polymer} = 2$ g/L. In terms of sensitivity of detection in indirect UV mode, it is thus interesting to know how the time-corrected peak area (CA) of a copolymer varies with f at a constant mass concentration. Combining eqs 18 and 10 leads to

$$CA = \alpha_S C_{M,1} = z_1 \alpha_A k_A \frac{f C_{m,polymer}}{f M_1 + (1-f) M_2} \tag{19}$$

For $f < f_{crit}$, CA scales as $k_A F_1$ since α_A and $C_{m,polymer}$ are constant and $z_1 = 1$. CA should increase with f because F_1 increases with f and k_A drops slightly with f compared to the increase of F_1. For $f > f_{crit}$, CA scales as $F_1/f \sim 1/(fM_1 + (1-f)M_2)$, since α_A, $C_{m,polymer}$, and k_A are constant. Thus, CA should decrease with f for $f > f_{crit}$. Therefore, CA is theoretically expected to pass through a maximum for $f = f_{crit}$. Figure 4 presents the variation of the theoretical (solid line) and experimental (square) values of CA according to f. Experimental values of CA (square) were determined from the electropherograms presented in Figure 1 but using a time-scale on the x-axis. Peak areas (in mAU·s) were corrected by migration times to account for different migration velocities of the sample bands. Theoretical CA values were determined from theoretical values of z_1 based on Manning theory and experimental values of α_A and k_A. Experimentally, CA increases with f for $f < f_{crit}$ in good agreement with the theoretical expectations. However, slightly lower values were experimentally obtained for $f < f_{crit}$. This is due to lower experimental z_1 values as already discussed. For $f > f_{crit}$, as expected, CA decreases with f, and experimental data are in good agreement with theoretical expectations.

4.4. Determination and Comparison of the Effective Charge Density (f_{eff}). From experimental values of z_1, effective charge densities f_{eff} of PAMAMPS copolymers were calculated according to eq 14. Effective charge densities were also determined for other polyelectrolytes such as PDADMAC, PMAA, and PAA homopolymers. All experimental values are listed in Table 1. Overall, experimental f_{eff} values are close to theoretical ones. For vinyl homopolymers, the effective charge

Table 1. Values of Chemical Charge Density (f), Charge Density Parameter (ξ), Effective Electrophoretic Mobility (μ_S), Transfer Ratio (TR), Mobility Ratio (k_A), Experimental Effective Charge per Monomer (z_1), and Effective Charge Density (f_{eff}) for All the Polyelectrolytes Studied in This Work[a]

samples		f	ξ	μ_S[b]	TR	k_A	z_1	$f_{eff,exp}$[c]	$f_{eff,theo}$
homopolymers	PAMPS	1	2.88	−38.3	0.31	0.87	0.35	0.35± 0.01	0.36
	PAA	1	2.88	−38.66	0.29	0.87	0.33	0.33 ± 0.03	0.36
	PMAA	1	2.88	−38.25	0.35	0.87	0.40	0.40 ± 0.02	0.36
	PDADMAC	1	1.44	43.05	0.62	0.94	0.66	0.66 ± 0.01	0.50−1
statistical copolymers	PAMAMPS 3%	0.03	0.08	−11.43	1.17	1.75	0.75	0.023 ± 0.002	0.03
	PAMAMPS 10%	0.1	0.28	−23.3	0.87	1.11	0.78	0.079± 0.010	0.10
	PAMAMPS 20%	0.2	0.57	−32.64	0.74	0.94	0.79	0.16 ± 0.02	0.20
	PAMAMPS 30%	0.3	0.86	−34.28	0.74	0.92	0.80	0.24 ±0.01	0.30
	PAMAMPS 55%	0.55	1.58	−39.28	0.53	0.86	0.60	0.33 ± 0.01	0.36
	PAMAMPS 85%	0.85	2.44	−39.24	0.37	0.86	0.42	0.35 ±0.02	0.36
diblock copolymers	PMAA−PEO	0.16	0.46	−22.16	0.33	1.15	0.28	0.046 ± 0.016	0.05
	PAA−PEO	0.58	1.68	−34.29	0.32	0.92	0.35	0.20± 0.02	0.20

[a] Electrophoretic conditions for PAMAMPS copolymers: Fused silica capillary, 50 μm i.d. × 33.5 cm (effective length, 25cm). Electrolytes: 12 mM ammediol, 6 mM *p*-anisic acid, pH = 8.8 (indirect UV detection) or 12 mM ammediol, 6 mM acetic acid, pH = 8.8 (direct UV detection for the measurement of α_a). Applied voltage: +10 kV. Hydrodynamic injection: 17 mbar, 5 s (sample) + 10 mbar, 3 s (buffer). UV detection at 254 nm. Temperature: 25 °C. Electrophoretic conditions for PMAA and PAA homopolymers and diblock copolymers: Fused silica capillary, 50 μm i.d. × 58.5 cm (effective length, 50 cm). Applied voltage: +20 kV. UV detection at 248 nm. Others conditions as for PAMAMPS copolymers. Electrophoretic conditions for PDADMAC homopolymer: didodecyldimethylammonium bromide (DDAB) coated capillary, 50 μm i.d. × 33.5 cm (effective length, 25cm). Electrolytes: 6 mM creatinine, 12 mM H_3PO_4, pH = 2.5 (indirect UV detection) or 6 mM NaH_2PO_4, 12 mM H_3PO_4, pH = 2.5 (direct UV detection for the measurement of α_a). Applied voltage: −10 kV. Hydrodynamic injection: 17 mbar, 5 s (sample) + 10 mbar, 3 s (buffer). UV detection at 191 nm. Temperature: 25 °C. The chemical charge density of all copolymer samples was determined by ^{1}H NMR. The composition of PAA−PEO was determined by acido-basic titration. See details in the text for the determination of the different parameters. [b] In 10^{-5} cm^2 V^{-1} s^{-1}. [c] Standard errors calculated from the linear fit using the Origin software.

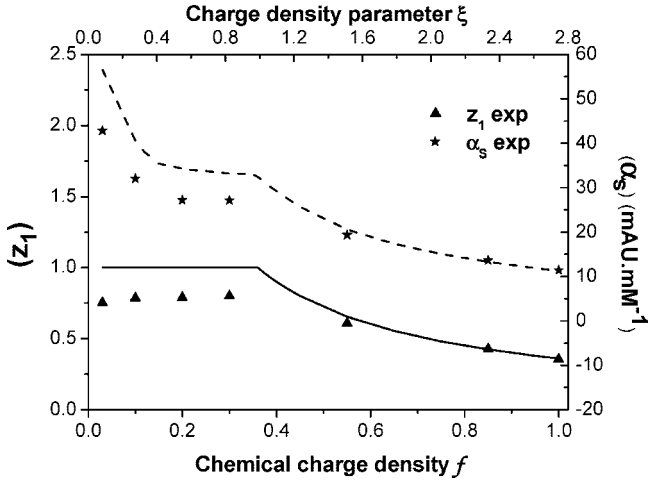

Figure 3. Variation of the effective charge per AMPS monomer z_1 and the sensitivity of detection α_S according to the chemical charge density f or the charge density parameter ξ. Electrophoretic conditions as in Figure 1.

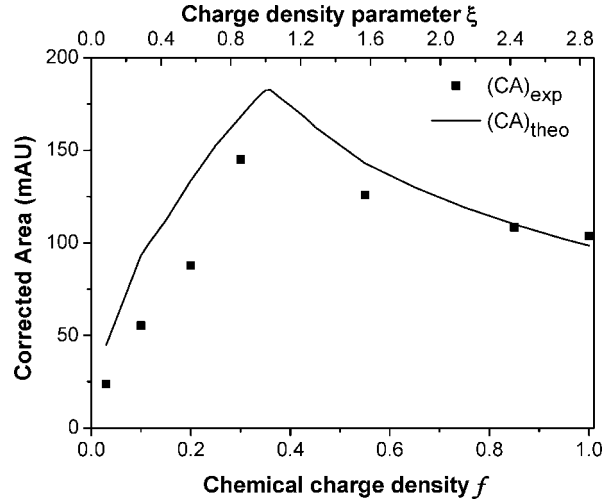

Figure 4. Variation of the time-corrected peak area of the PAMAMPS according to the chemical charge density f at constant mass concentration in copolymer. Electrophoretic conditions as in Figure 1. Experimental values are derived from the electropherograms presented in Figure 1 ($C_{m,polymer}$= 2 g/L). The solid line corresponds to the "theoretical" CA given by eq 19 with z_1 as predicted by the Manning theory.

density measured by indirect UV detection (0.35 for PAMPS and 0.33 for PAA) is in very good agreement with the Manning theory (0.36). For PMAA, the experimental value of f_{eff} (0.40) remains close to the expected value. Regarding the PDADMAC homopolymer, the effective charge density was expected to be much higher than for a vinyl polyelectrolyte because the distance b between charged monomers is higher. Different values of b are given in the literature: Mende et al.[4] used a value of b = 0.5 nm, which leads to $f_{eff,theo}$ = 0.70, while Carriere et al.[56] reported b = 0.45 nm ($f_{eff,theo}$ = 0.63) and Mattison et al.[1] used $b \sim 0.7$ nm ($f_{eff,theo} \sim 1$). In this work, the measurement of the effective charge density for the PDADMAC leads to a value of $f_{eff,exp}$ = 0.66 (b = 0.47 nm), which seems reasonable. This may reflect the "crumpled" nature of PDADMAC (rotations around the noncyclic C−C bonds tend to make the rings alternate).

For statistical PAMAMPS copolymers, it clearly appears from Table 1 that experimental values are in relatively good agreement with the theoretical ones. Figure 5 allows a better comparison by plotting on the same figure the variation of the effective charge density and the effective mobility as a function of f. Both two parameters tend to level off above f_{crit}. However, with the f_{eff} parameter, one can compare to the theory not only the overall curve shape as for the mobility curve but also the absolute value of this parameter. Above f_{crit}, effective charge densities are in very good agreement with the theoretical values. For the 20% and 30% PAMAMPS copolymers, experimental f_{eff} values seem to be slightly lower than theoretical expectations, but this could be explained by the presence of AMPS sequences in the copolymer chain, as discussed earlier. This result also suggests that, reversely, the determination of the effective charge by indirect UV detection CE should help to identify the presence of sequences of charged monomers in statistical copolymers.

To confirm that this approach can be used for characterizing the macromolecular architecture (or the monomer sequence in the chain), let us consider the case of two copolymers having the same chemical charge density (f = 0.3) but with different repartitions of the monomers as schematically depicted in Figure 6. One is a diblock copolymer (A), and the other one is a

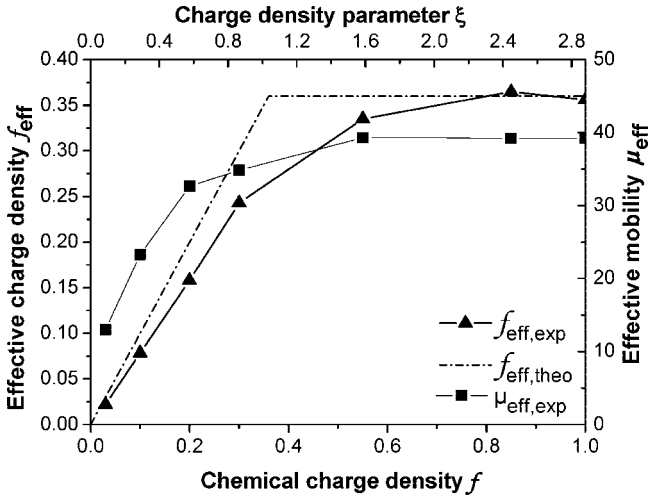

Figure 5. Variation of the effective mobility and the effective charge density f_{eff} of PAMAMPS copolymers according to the chemical charge density f (or charge density parameter ξ). Electrophoretic conditions as in Figure 1.

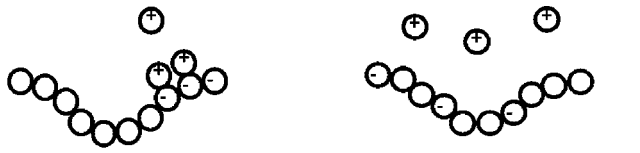

A . Diblock copolymer $f = 0.3$ B. Statistical copolymer $f = 0.3$

Figure 6. Schematic representation of diblock and statistical vinyl copolymers having the same chemical charge density ($f = 0.3$). There is no counterion condensation for the statistical copolymer, while the polyelectrolyte part of the diblock copolymer is partially condensed. The effective charge density is higher for the statistical copolymer ($f_{eff} = 0.3$) than for the diblock copolymer ($f_{eff} = 0.11$).

statistical copolymer (B). For vinyl copolymers at $f = 0.3$, the statistical copolymer is expected to be not condensed, while for the polyelectrolyte block of the diblock copolymer, counterion condensation is expected to occur. Therefore, for the statistical copolymer f_{eff} should be close to 0.3, while for the diblock copolymer f_{eff} should be equal to $0.36 \times 0.3 = 0.11$. Although the variation of the effective charge density with f levels off for vinyl statistical copolymers above f_{crit} (see Figure 5), it should increase linearly for diblock copolymers. The difference in effective charge between the two kinds of copolymers is given by

$$f_{eff,stat} - f_{eff,diblock} = f(1 - f_{crit}) \qquad \text{for } f < f_{crit} \tag{20}$$

and

$$f_{eff,stat} - f_{eff,diblock} = f_{crit}(1 - f) \qquad \text{for } f > f_{crit} \tag{21}$$

This difference in effective charge density passes through a maximum equals to $f_{crit}(1 - f_{crit}) = 0.23$ for $f = f_{crit}$, which corresponds to a difference of 64% in effective charge density between the two kinds of copolymers. Experimentally, since PAMAMPS diblock copolymers were not available, the polymer effective charge was determined for two diblock copolymers of PAA-*b*-PEO and PMAA-*b*-PEO having respectively chemical charge densities f of 0.58 and 0.16. The calibration curves (as in Figure 2) of the block copolymers should be identical to the PAMPS homopolymer. However, as mentioned in the text, the block copolymers have been characterized on a longer capillary than the PAMAMPS copolymers. Experimental conditions are not exactly the same (such as the injected volume for instance), and therefore the direct comparison on the same plot (Figure 2) is not possible. As shown in Table 1, there is a very good agreement between the experimental and theoretical values of f_{eff} for the two diblock copolymers. The comparison between the effective charge density f_{eff} obtained by this method and the chemical charge density f (obtained from NMR) allows to get information on monomers repartition along polyelectrolyte chains.

5. Conclusion

The determination of the sensitivity of detection in indirect UV detection is a simple and straightforward method in order to measure the effective charge density of polyelectrolytes. Contrary to other electrophoretic methods generally used for monitoring changes in effective charge, this method is based on the measurement of peak areas (sensitivity of detection) and not on the determination of migration times (i.e., effective mobility). The strength of this approach is that it gives a direct access to the effective charge density. Experimental results obtained for various vinyl copolymers are in relatively good agreement with the Manning theory. This approach is of great interest for the polymer chemist since it can be used for characterizing macromolecular architectures from the comparison of the experimental effective charge density with theoretical values derived from Manning theory. For instance, it has been demonstrated in this work that it is possible to distinguish a diblock copolymer from a statistical copolymer having the same chemical charge density by the experimental measurement of their effective charge densities. Besides the interest of this method for the characterization of polymer architecture, this technique can be used for the measurement of effective charge densities of (bio)macromolecules in different environments. Knowing the importance of electrostatic interactions in biological systems, this approach should likely represent a new opportunity to study subtle effects (such as the nature of counterions) by measuring the effective charge of the ionic partners involved in biological interactions.

Acknowledgment. We are thankful to Marvin Celle for the synthesis of the PAMAMPS ($f = 0.3$) copolymer.

References and Notes

(1) Mattison, K. W.; Dubin, P. L.; Brittain, I. J. *J. Phys. Chem. B* **1998**, *102* (19), 3830–3836.
(2) Gao, J. Y.; Dubin, P. L.; Muhoberac, B. B. *J. Phys. Chem. B* **1998**, *102* (28), 5529–5535.
(3) Zhang, H.; Dubin, P.; Ray, J.; Manning, G.; Moorefield, C.; Newkome, G. *J. Phys. Chem. B* **1999**, *103* (13), 2347–2354.
(4) Mende, M.; Petzold, G.; Buchhammer, H.-M. *Colloid Polym. Sci.* **2002**, *280* (4), 342–351.
(5) Radtchenko, I. L.; Sukhorukov, G. B.; Leporatti, S.; Khomutov, G. B.; Donath, E.; Möhwald, H. *J. Colloid Interface Sci.* **2000**, *230* (2), 272–280.
(6) Lee, S. H. *Polymer. J.* **2000**, *32* (9), 716.
(7) Petzold, G.; Nebel, A.; Buchhammer, H. M.; Lunkwitz, K. *Colloid Polym. Sci.* **1998**, *276*, 125.
(8) Kramer, G.; Buchhammer, H. M.; Lunkwitz, K. *J. Appl. Polym. Sci.* **1997**, *65*, 41.
(9) Baccile, N.; Reboul, J.; Blanc, B.; et al. *Angew. Chem., Int. Ed.* **2008**, *47* (44), 8433–8437.
(10) Buchhammer, H. M.; Petzold, G.; Lunkwitz, K. *Colloid Polym. Sci.* **2000**, *278*, 841.
(11) Decher, G. *Science* **1997**, *277* (5330), 1232–1237.
(12) Engelhardt, H.; Martin, M. *Adv. Polym. Sci.* **2004**, *165*, 211–247.
(13) Cottet, H.; Gareil, P. In *CE from Small Ions to Macromolecules*; Schmitt-Kopplin, P., Ed.; Serie Methods in Molecular Biology, Molecular Medicine and Biotechnology; Humana Press: Totowa, NJ, 2008; pp 541−567.
(14) Cottet, H.; Biron, J. P. *Macromol. Chem. Phys.* **2005**, *206* (6), 628–634.
(15) Cottet, H.; Biron, J. P.; Taillades, J. *J. Chromatogr. A* **2004**, *1051* (1−2), 25–32.
(16) Hoagland, D. A.; Smisek, D. L.; Chen, D. Y. *Electrophoresis* **1996**, *17* (6), 1151–1160.

(17) Manning, G. S. *J. Chem. Phys.* **1969**, *51*, 924.
(18) Gao, J. Y.; Dubin, P. L.; Sato, T.; Morishima, Y. *J. Chromatogr. A* **1997**, *766* (1−2), 233–236.
(19) Staggemeier, B.; Huang, Q. R.; Dubin, P. L.; Morishima, Y.; Sato, T. *Anal. Chem.* **2000**, *72* (1), 255–258.
(20) Zhang, B.; Hattori, T.; Dubin, P. L. *Macromolecules* **2001**, *34* (19), 6790–6794.
(21) Oudhoff, K. A.; Buijtenhuijs, F. A.; Wijnen, P. H.; Schoenmakers, P. J.; Kok, W. T. *Carbohydr. Res.* **2004**, *339* (11), 1917–1924.
(22) Pieric, I. M.; Rivas, B. L.; Pooley, A.; et al. *Bol. Soc. Chil. Quim.* **1999**, *44*, 345–350.
(23) Popov, A.; Hoagland, D. A. *J. Polym. Sci., Part B: Polym. Phys.* **2004**, *42* (19), 3616–3627.
(24) Essafi, W.; Lafuma, F.; Williams, C. E. *Eur. Phys. J. B* **1999**, *9*, 261–266.
(25) Von Klitzing, R.; Kolaric, B.; Jaeger, W.; Brandt, A. *Phys. Chem. Chem. Phys.* **2002**, *4*, 1907–1914.
(26) Pochard, I.; Couchot, P.; Foissy, A. *Colloid Polym. Sci.* **1998**, *276* (12), 1088–1097.
(27) Manning, G. S. *Polyelectrolytes*; Reidel: Dordrecht, 1974.
(28) Rinaudo, M.; Milas, M. *Chem. Phys. Lett.* **1976**, *41*, 456–459.
(29) Joshi, Y. M.; Kwak, J. C. T. *J. Phys. Chem.* **1979**, *83*, 1978–1983.
(30) Rios, H. E.; Gamboa, C.; Ternero, G. *J. Polym. Sci., Part B* **1991**, *29*, 805–809.
(31) Nordmeier, E. *Polym. J.* **1994**, *26*, 539–550.
(32) Nagaya, J.; Minakata, A.; Tanioka, A. *Langmuir* **1999**, *15*, 4129–4134.
(33) Wandrey, C.; Hunkeler, U.; Jaeger, W. *Macromolecules* **2000**, *33*, 7136–7143.
(34) Essafi, W. PhD Thesis, University of Paris 6 (France), **1996**.
(35) Wang, J. H. *J. Am. Chem. Soc.* **1951**, *73*, 510.
(36) Manning, G. S. *J. Chem. Phys.* **1981**, *85*, 1506.
(37) Strauss, U. P.; Woodside, D.; Winemann, P. *J. Phys. Chem.* **1957**, (61), 1353.
(38) Böhme, U.; Scheler, U. *Colloids Surf., A* **2003**, *222* (1−3), 35–40.
(39) Böhme, U.; Scheler, U. *Chem. Phys. Lett.* **2007**, *435* (4−6), 342–345.
(40) Böhme, U.; Scheler, U. *J. Colloid Interface Sci.* **2007**, *309* (2), 231–235.
(41) Long, D.; Viovy, J.-L.; Ajdari, A. *J. Phys.: Condens. Matter* **1996**, *8* (47), 9471–9475.
(42) Rintoul, I.; Wandrey, C. *Macromolecules* **2005**, *38* (19), 8108–8115.
(43) Pyun, C. W. *J. Polym. Sci., Part A* **1970**, *8*, 1111.
(44) Igarashi, S. *J. Polym. Sci., Part B* **1963**, *1*, 359.
(45) Liaw, D. J.; Huang, C. C.; Sang, H. C.; Wu, P. L. *Polymer* **2000**, *41*, 6123–6131.
(46) Hjerten, S.; Elenbring, K.; Kilar, F.; Liao, J.; Chen, A. J. C.; Siebert, C. J.; Zhu, M. *J. Chromatogr.* **1987**, *403*, 47.
(47) Kohlraush, F. *Ann. Phys.* **1897**, *62*, 209.
(48) Johns, C.; MAcka, M.; Haddad, P. R. *Electrophoresis* **2003**, *24*, 2150–2167.
(49) Doble, P.; Andersson, P.; Haddad, P. R. *J. Chromatogr. A* **1997**, *770* (1−2), 291–300.
(50) Charmot, D.; Corpart, P.; Michelet, D.; Zard, S.; Biadatti, T. Rhodia chimie WO 98/58974, **1998**.
(51) Charmot, D.; Corpart, P.; Adam, H.; Zard, S. Z.; Biadatti, T.; Bouhadir, G. *Macromol. Symp.* **2000**, *150*, (23−32).
(52) Reboul, J.; Nugay, T.; Lacroix-Desmazes, P.; In, M.; Gérardin, C. *Polym. Prepr.* **2008**, *49* (2), 316–317.
(53) Feng, X. H.; Dubin, P. L.; Zhang, H. W.; Kirton, G. F.; Bahadur, P.; Parotte, J. *Macromolecules* **2001**, *34* (18), 6373–6379.
(54) McCormick, C. L.; Chen, G. S. *J. Polym. Sci., Part B* **1982**, *20*, 817–838.
(55) Travas-Sejdic, J.; Easteal, A. *J. Appl. Polym. Sci.* **2000**, *75*, 619–628.
(56) Carrière, D.; Dubois, M.; Schönhoff, M.; Zemb, T.; Möhwald, H. *Phys. Chem. Chem. Phys.* **2006**, *8*, 3141–3146.

MA8025095